GROUND VIBRATIONS AND TILTS

Hideo Hanada
National Astronomical Observatory, Mizusawa, Iwate, JAPAN

1. INTRODUCTION

We cannot avoid effects of ground vibrations or tilts so far as we make some kind of precise experiments on the earth. The attraction of the Sun and the Moon periodically change positions, tilts and strains of the ground with various modes (Earth tides), ocean waves cause ground vibrations (microseisms) with periods ranging from about 2 to 10 seconds according to geology under ground, and human activities such as traffic also cause ground vibrations (cultural noises) with periods from about 0.05 to 0.2 seconds. Winds, water flows, earthquakes and volcanoes also induce vibrations although they may be very weak or local. Vibrations observed on the Earth have various frequencies ranging from 10^{-8} to 10^{2} Hz. From the point of view of spatial pattern, ground vibrations and tilts have various characteristic lengths or wavelengths being related to their periods.

2. EARTH TIDES

The solid Earth always receives attraction from the Sun, the Moon and the other planets and change its shape due to them. This is called Earth tides. Since the celestial bodies are moving regularly following a certain law, variation of the potential generated by the attraction is perfectly described by a trigonometrical function with many different amplitudes, frequencies and phases. The Earth tides cause ground vibrations and tilts although their frequencies are very low.

With spherical coordinates in which r be radius, θ co-latitude, λ geocentric longitude and O the center, the attractive force acting at O and $\mathrm{P}(r,\theta,\lambda)$ due to a celestial body B of mass M at Q(r',θ',λ') is expressed as

$$f_r(O) = \frac{GM}{r'^2}\cos\alpha, \tag{1}$$

$$f_r(P) = \frac{GM}{l^2}\sin\beta = \frac{GM}{r'^2 + r^2 - 2r'r\cos\alpha}\cos\beta, \tag{2}$$

where l is the distance between P and Q, α the angle between OQ and OP, β the angle between PQ and PO, and the subscript r means the OP direction (see Figure 1). The difference of the forces acting on P from that on O are

$$\Delta f_r(P) = f_r(P) - f_r(O) = -GM\left[\frac{r'\cos\alpha - r}{(r'^2 + r^2 - 2r'r\cos\alpha)^{3/2}} - \frac{\cos\alpha}{r'^2}\right], \tag{3}$$

$$\Delta f_t(P) = f_t(P) - f_t(O) = GM\sin\alpha\left[\frac{r'}{(r'^2 + r^2 - 2r'r\cos\alpha)^{3/2}} - \frac{1}{r'^2}\right], \tag{4}$$

where the subscript t means the force in the direction on the plane OPQ and perpendicular to OP, and we used the relations

$$r'\sin\alpha = l\sin\beta, \tag{5}$$

$$r'\cos\alpha = r + l\cos\beta, \tag{6}$$

$$l^2 = r'^2 + r^2 - 2r'r\cos\alpha. \tag{7}$$

Equations (3) and (4) express the distribution of the tidal forces relative to those acting on the center. They can be also derived by differentiating the potential with respect to r and α. The tidal potential is in the form

$$\begin{aligned} &= GM\left(\frac{1}{\sqrt{r'^2 + r^2 - 2r'r\cos\alpha}} - \frac{r\cos\alpha}{r'^2} - \frac{1}{r'}\right) \\ &= \frac{GM}{r'}\sum_{n=2}^{\infty}\left(\frac{r}{r'}\right)^n P_n(\cos\alpha). \end{aligned} \tag{8}$$

The second and the third terms in the parenthesis are necessary in order that the tidal potential U and its derivative $\partial U/\partial r'$ should be zero at the center 0. If we omit the terms higher than second order of r'/r, (8) can be approximated by

$$U = \frac{GMr^2}{2r'^3}(3\cos^2\alpha - 1). \tag{9}$$

By applying a formula of the spherical triangle:

$$\begin{aligned} \cos\alpha &= \cos\theta\cos\theta' + \sin\theta\sin\theta'\cos(\lambda - \lambda') \\ &= \cos\theta\sin\delta + \sin\theta\cos\delta\cos H, \end{aligned} \tag{10}$$

(9) becomes

$$U = \frac{3GMr^2}{4r'^3}\left[\sin^2\theta\cos^2\delta\cos 2H + \sin 2\theta\sin 2\delta\cos H + 3\left(\cos^2\theta - \frac{1}{3}\right)\left(\sin^2\delta - \frac{1}{3}\right)\right], \tag{11}$$

where δ and H are the declination and the hour angle (angular distance west of a celestial meridian) of the celestial body, respectively. Precise harmonic development of the tide-generating potential was newly given by Tamura [1].

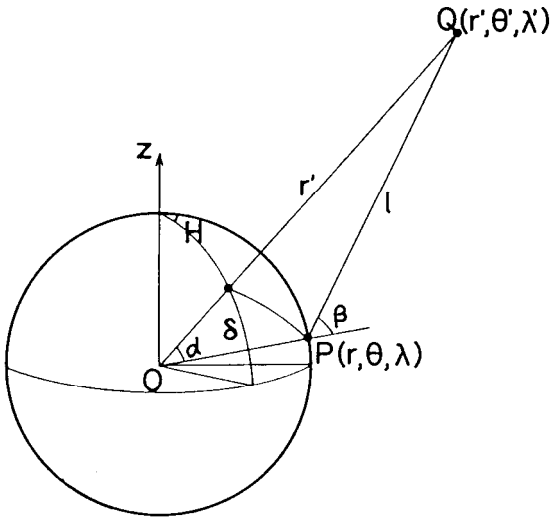

Fig.1 The Earth and a celestial body in the equatorial coordinate.

Displacement and tilt of the Earth's surface due to the Earth tides are estimated by using the tidal potential. Radial displacement u_r, southward displacement u_θ and eastward displacement u_λ are obtained by

$$u_r = (h/g)U, \tag{12}$$

$$u_\theta = (l/g)\partial U/\partial\theta, \tag{13}$$

$$u_\lambda = [l/(g\sin\theta)]\partial U/\partial\lambda, \tag{14}$$

where g is gravitational acceleration, h and l are Love and Shida numbers, respectively. Tilt in north and south (NS) component t_θ and that in east and west (EW) component t_λ, on the other hand, are obtained by

$$t_\theta = -[(1+k-h)/(rl)]u_\theta = -[(1+k-h)/(rg)]\partial U/\partial\theta, \tag{15}$$

$$t_\lambda = -[(1+k-h)/rl]u_\lambda = -[(1+k-h)/(rg\sin\theta)]\partial U/\partial\lambda, \tag{16}$$

where k is also Love number and positive values of t_θ and t_λ mean descent of northward and westward ground, respectively.

The first term in the right side of (11) represents the tidal component which varies with a period of about 12 hours according to cos $2H$ and has the name of semidiurnal tide. Its amplitude is maximum at the equator and is zero at the poles for arbitrary declination of the celestial body. This term is also called sectorial function since its spatial distribution is equivalent to that of the spherical harmonic coefficient of P_{22} which has two nodal lines of meridians separated by 90 degrees and the region surrounded by them is like a sector [2]. The M_2 component, which is produced by a fictitious Moon revolving along a circular orbit in the plane of the equator with a velocity equal to the mean velocity of the real Moon, has a period of 12.4167 hours and has the largest amplitude. The expected amplitude of vertical, NS and EW displacements due to the M_2 component at the latitude of 35° N are about 98mm, 19mm and 33mm, and NS and EW tilts are 2.5 x 10^{-8} rad and 4.4 x 10^{-8} rad, respectively. The S_2 component which is produced by a fictitious Sun in a circular and equatorial orbit with the mean velocity of the real Sun, on the other hand, has a period of exactly 12 hours and amplitudes of vertical, NS and EW displacements are about 46mm, 9mm and 16mm, and NS and EW tilts are 1.2 x 10^{-8} and 2.0 x 10^{-8}, respectively, at 35° N.

The second term in (11) varies with a period of about 24 hours according to cos H and has the name of diurnal tide or tesseral function [2]. The distribution is characterized by two nodal lines, one is the equator and another is a meridian, and is equivalent to the spherical harmonic coefficient of P_{21}. The amplitude has its maximum at the latitudes of 45° N and 45° S and is always zero at the equator and the poles. There are major components of K_1 and O_1 in the diurnal tide which have periods of one sidereal day (23.935 hours) and 25.819 hours, respectively. The three component, (vertical, NS, EW), displacements have amplitudes of (80 mm, 8mm, 20mm) as to Kr and (57mm, 6mm, 14mm) as to O_1, and two component (NS, EW) tilts have (1.1 x 10^{-8}, 1.8 x 10^{-8}) as to K_1 and (7.6 x 10^{-9}, 1.3 x 10^{-8}) as to O_1, respectively, at 35° N.

The third term, which is called zonal function or long period tide, does not varies according to the Earth's rotation but varies according to the declination of the celestial body and has a period of about 14 or 28 days with respect to the Moon and about six months or one year with respect to the Sun. This shows a zonal distribution with two nodal lines of parallels 35°16′ N and 35°16′ S, and the amplitude has its maximum at the equator. The amplitude is not zero at the poles unlike the other terms. The fundamental lunar origin component is M_f which is caused by variation of the declination and has a period of 13.66 days and the elliptical orbit of the Moon generates the component M_m which has a period of 27.55 days. The Sun also cause the long period tides corresponding to those of the Moon origin. They are S_a and S_{sa} components and have periods of 365.26 days and 182.62 days, respectively. The amplitudes are one order of magnitude less than those of the major components in diurnal and semidiurnal tides and they have no EW

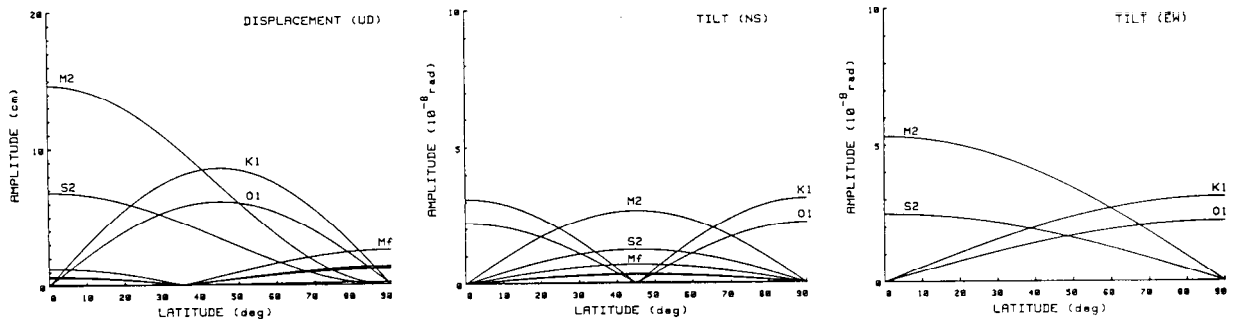

Fig.2 Amplicatude variation of principal tidal waves as a function of latitude for vertical displacements (left), NS tilts (middle) and EW tilts (right).

component. The three component displacements as to M_f, M_m, S_a, and S_{Sa} at 35° N are (0.2mm, 5.0mm, 0mm), (0.09mm, 2.6mm, 0mm), (0.01mm, 0.37mm, 0mm) and (0.08mm, 2.3mm, 0mm), and NS component tilts as to the four long period tides are 6.5 x 10^{-9}, 3.4 x 10^{-9}, 4.8 x 10^{-10} and 3.0 x 10^{-9}, respectively. Amplitude variation of principal tidal waves as a function of latitude for vertical displacements, NS tilts and EW tilts are shown in Figure 2.

3. MICROSEISMS

The equation of motion of an elastic solid medium is written

$$\rho \frac{\partial^2 \mathbf{u}}{\partial t^2} = (\lambda + 2\mu)\mathrm{grad} \cdot \mathrm{div}\mathbf{u} - \mu \mathrm{rot} \cdot \mathrm{rot}\mathbf{u} + \rho \mathbf{f}, \tag{17}$$

where ρ is density of the medium, $\mathbf{u}$ displacement vector, λ and μ are Lamé constants and $\mathbf{f}$ body force, respectively [3]. The is displacement vector $\mathbf{u}$ is usually written in the form

$$\mathbf{u} = \mathrm{grad}\phi + \mathrm{rot}\mathbf{A}, \tag{18}$$

with a scalar potential 4 and a vector potential A, where $\mathrm{div}\mathbf{A} = 0$. We consider the case of the equilibrium of an isotropic solid medium under no body force. Then (17) and (18) lead to wave equations

$$\nabla^2 \phi = \frac{1}{\alpha^2} \frac{\partial^2 \phi}{\partial t^2} \tag{19}$$

and

$$\nabla^2 \mathbf{A} = \frac{1}{\beta^2} \frac{\partial^2 \mathbf{A}}{\partial t^2}, \tag{20}$$

where $\alpha = \sqrt{(\lambda + 2\mu)/\rho}$ and $\beta = \sqrt{\mu/\rho}$.

Let the scaler potential ϕ and the vector potential $\mathbf{A}$ be functions of only the distance from a source r and time t. Then displacement vectors derived from the potentials ϕ and $\mathbf{A}$ in a spherical coordinate (r, θ, λ) are

$$\mathbf{u} = \mathrm{grad}\phi = (\partial\phi/\partial r, 0, 0), \tag{21}$$

$$r = \mathrm{rot}\mathbf{A} = [0, -\frac{1}{r}\frac{\partial}{\partial r}(rA_\lambda), \frac{1}{r}\frac{\partial}{\partial r}(rA_\theta)]. \tag{22}$$

General solutions for (19) and (20) are

$$\phi = \frac{1}{r}[f_1(r - \alpha t) + f_2(r + \alpha t)], \tag{23}$$

$$A_\theta = \frac{1}{r}[g_1(r - \beta t) + g_2(r + \beta t)], \tag{24}$$

$$A_\lambda = \frac{1}{r}[h_1(r - \beta t) + h_2(r + \beta t)], \tag{25}$$

with arbitrary functions *f, g* and *h*. Only the first terms in (23)-(25) represent real waves traveling in the direction of *r* decreasing. The displacement derived from ϕ by using (21) propagates with velocity α in *r* direction with only *r* component, which we call P wave (primary wave) or longitudinal wave. The displacements derived from **A,** on the other hand, propagate with velocity β in *r* direction with θ and λ components, which we call S wave (secondary wave) or transverse wave. We generically call P and S waves as body wave since they travel interior of the Earth.

In addition to the P and S waves, an elastic solid medium with a free surface can transmit two kinds of surface waves. We take a wave which progress in *x* direction with only x and *z* components under the free surface $z = 0$ and *z* in positive downward, Then **u** and **v** are functions of *x, z* and *t,* and the displacement vectors in a rectangular coordinate (x, y, z) are

$$\mathbf{u} = (u_x, u_y, u_z) = (\frac{\partial \phi}{\partial x}, 0, \frac{\partial \phi}{\partial z}), \tag{26}$$

$$\mathbf{v} = (v_x, v_y, v_z) = (\frac{\partial A_y}{\partial z}, 0, \frac{\partial A_y}{\partial x}). \tag{27}$$

We find solutions for a surface wave (Rayleigh wave) of

$$\phi = F_0 \exp[i(\omega t - kx) - pz], \tag{28}$$

$$A_y = G_0 \exp[i(\omega t - kx) - qz], \tag{29}$$

where $p = \sqrt{k^2 - (\omega/\alpha)^2}$ and $q = \sqrt{k^2 - (\omega/\beta)^2}$. Boundary condition is that there is no stress over the surface $z = 0$ and we have the relations

$$2ipkF_0 - (2k^2 - q^2)G_0 = 0, \tag{30}$$

$$(2k^2 - q^2)F_0 + 2iqkG_0 = 0, \tag{31}$$

The condition where F_0 and G_0 have non-zero solutions requires the following characteristic equation

$$(2k^2 - q^2)^2 - 4pqk^2 = 0. \tag{32}$$

Displacements derived from (26)-(31) are then

$$U_x = u_x + v_x = kF_0[\exp(-pz) - 2pq/(2k^2 - (\omega/\beta)^2)\exp(-qz)]\exp[i(\omega t - kx - \pi/2)], \tag{33}$$

$$U_z = u_z + v_z = kF_0[-(p/k)\exp(-pz) + 2kp/(2k^2 - (\omega/\beta)^2)\exp(-qz)]\exp[i(\omega t - kx)]. \tag{34}$$

We have the solution of $k = (\omega/\beta)\sqrt{(3 + \sqrt{3})/4}$ from (32) if we suppose that $\lambda = \mu$ and we get

$$\gamma_R = \omega/k = \beta\sqrt{4/(3 + \sqrt{3})}, \tag{35}$$

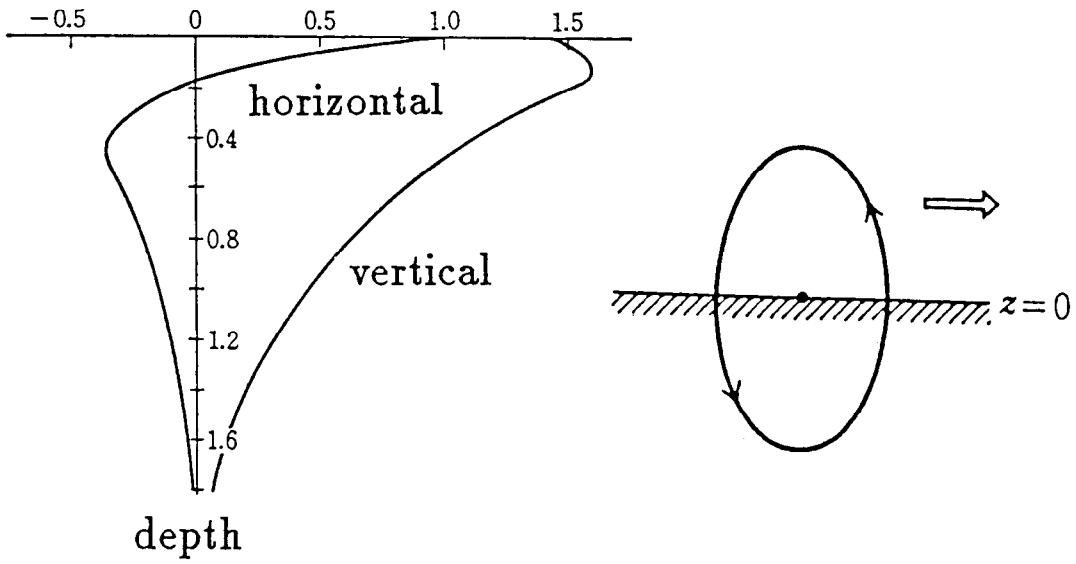

Fig.3 Variation of the displacement amplitudes of the Rayleigh wave with depth (left) and the pattern of its particle motion (right). The depth is normalized with the wavelength.

where γ_R is the velocity of the Rayleigh wave and we find γ_R is less than that of S wave velocity β. The coefficients $2pq/(2k^2-(\omega/\beta)^2)$ in (33), p/k and $2kp/(2k^2-(\omega/\beta)^2)$ in (34) take values of 0.57, 0.85 and 1.47, respectively. The motion at the surface is given by (33) and (34). The particles moves in ellipses and the amplitude of the vertical movement being about 1.5 times that of the horizontal at the surface. The amplitude ratio and the particle motion are shown in Figure 3.

There exists another type of surface wave, Love wave, under the condition where a surface layer of thickness H overlying a deep layer and the S wave velocity in the upper layer is smaller than that in the lower layer. It has horizontal displacements at right angle to the plane of propagation. The y component displacement is derived only from the potential **A:**

$$v = v_y = \frac{\partial A_x}{\partial z} - \frac{\partial A_z}{\partial x}. \tag{36}$$

We find solutions which satisfies (20):

$$v_1 = C\exp[i(\omega t - kx + s_1 z] + C\exp[i(\omega t - kx - s_1 z], \tag{37}$$

$$v_2 = D\exp[i(\omega t - kx) - s_2 z], \tag{38}$$

where $s_1 = \sqrt{(\omega/\beta_1)^2 - k^2}$, $s_2 = \sqrt{k^2 - (\omega/\beta_2)^2}$, and β_1 and β_2 are the S wave velocities in the upper and the lower layers, respectively. We can obtain the following relations under boundary conditions, 1) stress free at z = 0, 2)displacement is continuous at the boundary, 3) stress is continuous at the boundary,

$$D = 2C\cos(s_1 H)\cdot\exp(s_2 H), \tag{39}$$

$$\mu_1 s_1 \tan(s_1 H) = \mu_2 s_2, \tag{40}$$

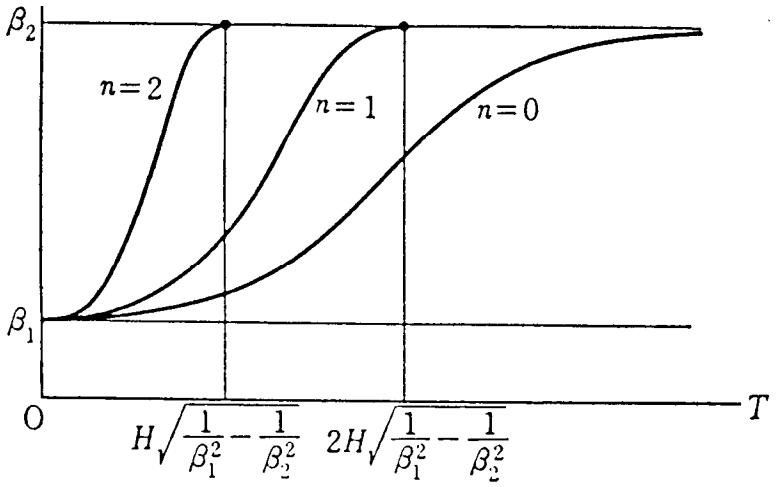

Fig.4 Variation of the velocity of the Love wave with its period as to fundamental (n=O), second harmonic (n= 1) and third harmonic (n=2) modes (dispersion curve).

where μ_1 and μ_2 are the Lame constants in the upper and the lower layers, respectively. Hence s_1 is real the condition for the velocity of the Love wave γ_L is

$$\beta_1 < \gamma_L < \beta_2, \tag{41}$$

The Love waves travel with velocity between that of the lower layer and that of the upper layer. The velocity of the Love wave γ_L is written as

$$\gamma_L = \omega/k, \tag{42}$$

By substituting $\omega = \beta_1\sqrt{s_1^2 + k^2}$ and $k = 2\pi/(\gamma_L T)$ we get

$$\gamma_L = 1/\sqrt{1/\beta_1^2 - (s_1 T/2\pi)^2}, \tag{43}$$

where T is period of the wave. This equation means that the velocity depends on the period. Figure 4 shows the relation between the velocity of the Love wave and its period.

The microseisms and the cultural noises travel in a ground surface layer with characteristics of combinations of Rayleigh and Love waves. Observations of microseisms in a frequency range from 1 to 200 Hz at Kakioka (Ibaragi, Japan) made by Akamatsu [4] suggested that high frequency microseisms (or cultural noises) consisted of Rayleigh waves for the reasons mentioned below. In order to study the short period microseisms, she settled a right angled triangle network of seismometers with the length of a side of about 10-50 m, and calculated cross-correlation coefficients of waves at two points. The direction of wave propagation and phase velocity were measured by using this network. The velocity of the microseisms in a frequency range from 1 to 10 Hz measured at several points in Hongo, Kokubunji and Tanashi (Tokyo, Japan) distributed in a range from about 200 to

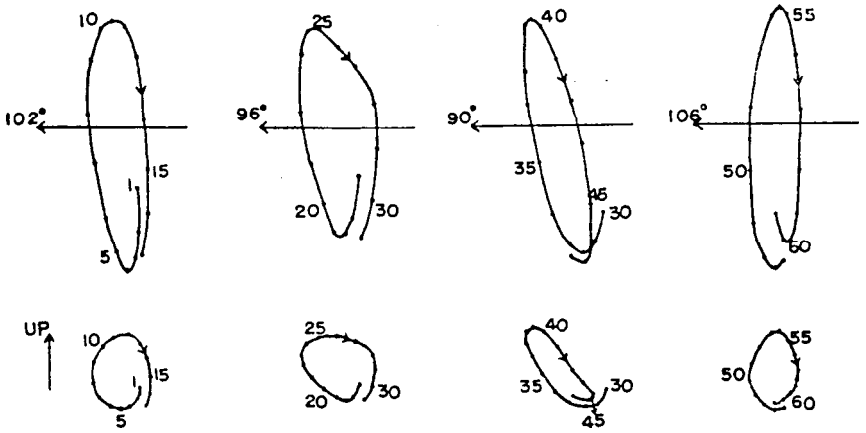

Fig.5 Orbital motions in the horizontal plane (upper) and the vertical plane (lower) of the microseisms observed at Tanashi city. The numbers along the orbits indicate time in 0.1 s unit (after Akamatsu [4]).

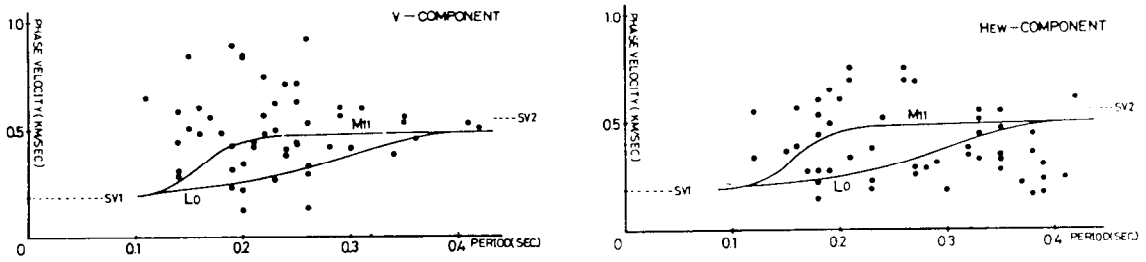

Fig.6 Relation between the phase velocity and the period (dispersion curve) of the microseisms observed at Hakodate city (after Nogoshi and Igarashi [5]).

600 m/s with wave lengths of from about 100 to 150 m [4]. The P wave velocity in loam like geology in Tokyo is about from 135 to 200 m/s with wave length of about 5 m. It is difficult to consider that the microseisms are the body wave such as P or S wave.

Synthesis of wave orbits was also made by using data obtained by the triangle network [4]. The orbit should be a straight line in the horizontal plane if the Love wave propagates in only one direction. The Rayleigh wave, on the other hand, propagates with elliptical orbits in a vertical plane. Figure 5 shows an example of orbits of the microseisms. They are interpreted as a combination of the Rayleigh and the Love waves propagating in some directions, since the orbits have the horizontal component about three times as large as the elliptical vertical one and they are not straight lines in horizontal plane.

The relation between phase velocity and period is also used as a proof of the surface waves. Nogoshi and Igarashi [5] investigated the propagation characteristics of microseisms with a frequency range from 1 to 20 Hz by using triangular networks. Figure 6 shows the relation between the phase velocity and the period of the microseisms observed at Hakodate (Hokkaido, Japan). W can see the characteristics of the dispersion curves of fundamental modes of the Rayleigh and the Love waves in the observed relations.

It is important to investigate the origin of the microseisms. General idea is that the microseisms originate in ocean waves and the cultural noises in human activities such as traffic. Santo [6,7] examined the microseisms by a synoptic method using the observational data at many stations over Japan. He showed 1) the microseismic storm occurs considerably later than the passing of the center of cyclone or typhoon, 2) the microseismic storm

TOC

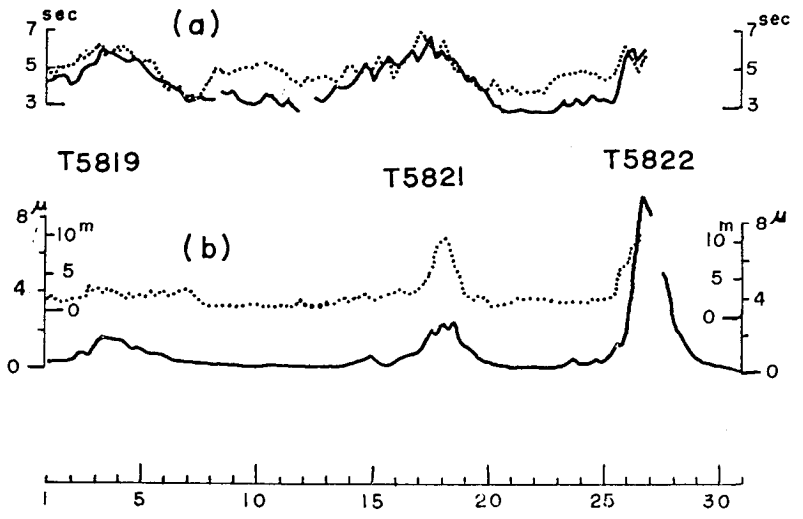

Fig.7 Comparison between amplitude of the microseisms (M) at Tsukuba and swell height (W) at Naarai (lower), and comparison of period of the microseisms (solid line) with half period of the swells (dotted line) as to the same stations (upper) (after Santo [7]).

also occurs when a strong cold front passes across Japan from west to east, 3) the direct cause of the microseisms is swells, 4) period of the microseisms is nearly equal to half the period of swells, 5) energy transformation from the swells to the microseisms takes place somewhere near the coast not in or around the center of the typhoon [6,7]. Figure 7 shows the comparison between amplitude of the microseisms (M) at Tsukuba (Ibaragi, Japan) and swell height (W) at Naarai (Ibaragi, Japan). Comparison of period of the microseisms with that of the swell of the same stations is also shown in the Figure.

REFERENCES

[1] Y. Tamura,"A Harmonic Development of the Tide-generating Potential," *Marees Terestres Bulletin d'Information*, 99(1987), pp.6813-6855.

[2] P. Melchior,"The Earth Tides," Pergamon Press, Oxford,(1966), pp.13-38.

[3] A. E. H. Love,"A Treatise on the Mathematical Theory of Elasticity," Dover Publications, New York,(1927), pp.293-309.

[4] K. Akamatsu,"On Microseisms in Frequency Range from 1 c/s to 200 c/s," *Bull. Earthq. Res. Inst., 39(1961),* pp.23-75.

[5] M. Nogoshi, T. Igarashi,"On the Propagation Characteristics of Microtremor," J. *Seis. Soc. Japan (Zisin),* 2nd Series, 23(1970), pp.264-280 (in Japanese).

[6] T. Santo,"Investigations into Microseisms Using the Observational Data of Many Stations in Japan (Part I)," *Bull. Earthq. Res. Inst., 37(1959),* pp.307-325.

[7] T. Santo,"Investigations into Microseisms Using the Observational Data of Many Stations in Japan (Part II)," *Bull. Earthq. Res. Inst.,* 37(1959), pp.483-494.